Are the western Mogollon-Datil mid-Cenozoic ash flows cogenetic? Pearce element ratios and isotopic aspects of the question

Michael Bikerman

1994, pp. 187-192. https://doi.org/10.56577/FFC-45.187

in:

Mogollon Slope (West-Central New Mexico and East-Central Arizona), Chamberlin, R. M.; Kues, B. S.; Cather, S. M.; Barker, J. M.; McIntosh, W. C.; [eds.], New Mexico Geological Society 45th Annual Fall Field Conference Guidebook, 335 p. https://doi.org/10.56577/FFC-45

This page is intentionally left blank to maintain order of facing pages.

ARE THE WESTERN MOGOLLON-DATIL MID-CENOZOIC ASH FLOWS COGENETIC? PEARCE ELEMENT RATIOS AND ISOTOPIC ASPECTS OF THE QUESTION

MICHAEL BIKERMAN
Department of Geology and Planetary Science, University of Pittsburgh, Pittsburgh, PA 15260

Abstract—The three major ash flows in the western Mogollon-Datil volcanic field, the Davis Canyon Tuff, Shelley Peak Tuff, and Bloodgood Canyon Tuff, and the flow-banded rhyolites with which they are associated, were produced in a period of about 1 Ma from two interlocking calderas — the Gila Cliff Dwellings (source of Davis Canyon and Shelley Peak Tuffs), and the Bursum (source of Bloodgood Canyon Tuff). Magmas parent to the tuffs could have been produced by assimilation of existing crust by a mantle-derived basaltic magma, and fractional crystallization of the resultant mix. Fractionation of pyroxene and plagioclase in varying proportions from more mafic magmas produced the present ash flows. The proportions calculated from the use of Pearce element ratios were 80:20 plagioclase:pyroxene for ash flows from the Gila Cliff Dwellings caldera and 55:45 for the Bursum caldera- derived Bloodgood Canyon Tuff.

INTRODUCTION

The western Mogollon-Datil volcanic field is dominated by outcrops of three widespread ash-flow tuffs. From the oldest to youngest these are the Davis Canyon Tuff, Shelley Peak Tuff and Bloodgood Canyon Tuff. As large scale extrusions of ash flows are commonly associated with calderas, these flows are tied to the Bursum caldera, roughly 45 km in diameter, and the slightly smaller Gila Cliff Dwellings caldera, located just to its east (Ratté et al., 1984; Elston, 1984; McIntosh et al., 1992). The ash flows have been dated by conventional K-Ar and fission tracks (Marvin et al., 1987), and more precisely by $^{40}Ar/^{39}Ar$ (McIntosh et al., 1991, 1992) as follows: Davis Canyon Tuff - 29.0 Ma; Shelley Peak Tuff - 28.1 Ma, and Bloodgood Canyon Tuff - 28.1 Ma. The ash flows are associated with their defluidized residues, the flow-banded rhyolites. Sr and Nd isotopic evidence (Bikerman, 1989; Bikerman et al, 1992) is consistent with an origin of the major ash flows by mixing of mantle-derived magma with Proterozoic upper crust in an assimilation and fractional crystallization (AFC) model (DePaolo, 1981).

Results of chemical analyses of Mogollon-Datil volcanic rocks were given by Elston and Northrup (1976), Ratté and Grotbo (1979), Bornhorst (1980, 1985) and Bikerman et al. (1992), whose values are used in the following discussion. In this paper the mineralogic changes in the evolving magma chamber purported to underlie the Bursum and Gila Cliff Dwellings calderas are examined using Pearce element ratios.

Pearce element ratios (PER) (Pearce, 1968) are petrogenetic modeling tools that use ratios of abundances of element(s) known to fractionate relative to some conservative parameter – the conserved parameter usually being a major element with an essentially unchanging composition in the evolving system. Most often these results are plotted against another similar ratio that uses the same denominator. The slope of the line through the data points reflects the stoichiometry of the fractionation (or addition) of material, with the original system controlling the intercept (Russell et al., 1990). For example, these authors used the ratios of 0.5(Mg+Fe)/Ti as the Y axis, and Si/Ti as the X axis in a test of an olivine fractionation hypothesis for variance within an Hawaiian lava. These PER axes are based on the concept that olivine fractionation will remove iron plus magnesium and silica from the melt in a 2:1 ratio. The 0.5 factor is used to get a straight line with a slope of one. Ti is used as the common denominator because it does not fractionate from a magma at low silica values. If the hypothesis is correct, then all the data points plot within experimental error of the olivine fractionation line. Similar plots can be used for fractionation of pyroxenes, feldspars, and other minerals, and have been used mostly in studies of mafic rocks. Valid trends have the additional requirements that the intercept not be zero (Pearce, 1987), and that the variance of ratios of conserved elements should not greatly exceed the experimental errors (Nicholls, 1988).

An interesting modification of PER use was by Bradshaw (1992), who adapted PERs for rhyolites and related high-silica rocks. The main change was the use of a trace element, Zr, as the common denominator. This was based on the observation that its fractionation as zircon is inhibited both by high temperature and presence of volatiles - both common factors in the magma chambers parent to ash flows.

In this study PERs using Zr (Bradshaw, 1992) as well as Cu, Ti, La and Ce as incompatible elements were calculated. All of these elements have essentially flat Harker plots of element (or oxide for TiO_2) abundances against SiO_2 (Figs. 1, 2) in the felsic range of silica contents. Flat Harker plots are used as a primary check on incompatibility. Mobile incompatible elements such as Ba and Rb were checked for their suitability, but as expected (Bradshaw, 1992), PER plots using these elements had considerable scatter, reflecting their mobility. Ni, Cr, V and Zn were checked, but yielded results similar to Cu. The technique used for elemental analyses was unlikely to dissolve zircons completely (Fabec, 1987, written commun.), so the Zr values given in Table 1 are for soluble Zr.

DATA

The chemical compositions, as oxide weight percents, used in the study are presented in Tables 1 and 2. PERs use element proportion

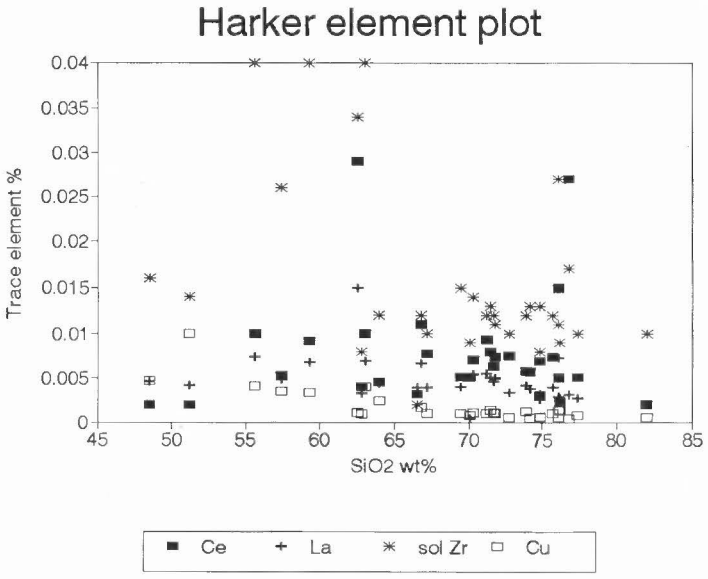

FIGURE 1. Harker element plots of Ce, La, sol Zr and Cu vs. SiO_2; symbols as shown on figure. Sol Zr is soluble zirconium under the analytical chemical technique used.

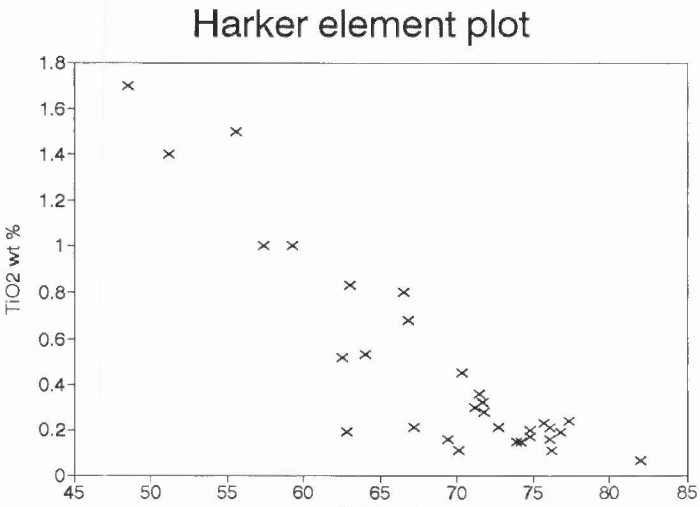

FIGURE 2. Harker element plot of TiO_2 vs. SiO_2

ratios in their calculations (Russell et al., 1990). These are obtained by multiplying the weight percent oxide by the number of cations in the oxide formula, then dividing by the molecular weight of the oxide.

The initial $^{87}Sr/^{86}Sr$ and $^{143}Nd/^{144}Nd$ ratios for the tuffs are 0.7089±0.0008 and 0.51227±0.00004 for the Davis Canyon Tuff; 0.7086±0.0004 and 0.51226±0.00004 for the Shelley Peak Tuff, and 0.7095±0.0006 and 0.51221±0.00004 for the Bloodgood Canyon Tuff, respectively; the initial $^{87}Sr/^{86}Sr$ for the flow-banded rhyolites ranged from 0.71003 for one with 32.8 ppm Sr, to high values of 0.71507 and 0.72872 for rocks with very low Sr contents of 6.2 and 4.7 ppm (Bikerman et al., 1992).

DISCUSSION

The three major ash flows erupted within a narrow interval in early Chattian (late Oligocene) time (McIntosh et al., 1992) from sources in the Gila Cliff Dwellings and Bursum calderas (Ratté et al., 1984). The short time span of the ash flow eruptions, similarity of isotopic ratios, and geographically limited possible source region, as delineated by the calderas, are consistent with eruption from a single evolving magma chamber. The Davis Canyon and Shelley Peak ash flows, which are probably from the Gila Cliff Dwellings caldera (Ratté et al., 1984), have identical $^{87}Sr/^{86}Sr$ isotopic ratios. These values are slightly lower than those of the Bloodgood Canyon Tuff, derived from the Bursum caldera. The difference could be caused by the additional million years or so of residence time in the magma chamber, which would cause an increase of *ca* 0.00001 in the $^{87}Sr/^{86}Sr$. Another possibility is that the portion of the magma chamber underlying the Bursum caldera might have encountered some more radiogenic country rock, giving rise to the slightly higher initial $^{87}Sr/^{86}Sr$ in the younger ash flow.

TABLE 1. Major element contents of rocks from the Mogollon-Datil volcanic field in weight percent.

Sample	SiO_2	TiO_2	Al_2O_3	Fe_2O_3	MnO	MgO	CaO	Na_2O	K_2O	P_2O_5
G-48	77.4	0.24	12.1	1.5	0.078	0.35	0.36	3.6	5.0	0.018
G-51	76.1	0.21	12.0	1.4	0.070	0.14	0.28	3.8	5.0	0.021
G-24	75.7	0.23	11.8	1.6	0.061	0.15	0.36	3.9	5.1	0.022
G-23	74.8	0.20	11.9	1.4	0.071	0.17	0.18	3.3	5.3	0.032
G-7	74.8	0.17	11.6	1.0	0.051	0.09	0.26	3.6	4.9	0.200
M-675	72.7	0.21	11.8	1.2	0.074	0.41	0.75	2.8	5.2	0.043
G-15B	71.8	0.28	14.5	1.7	0.054	0.31	1.00	3.9	5.1	0.077
G-15A	71.7	0.32	13.4	1.9	0.061	0.33	1.10	3.3	5.5	0.140
G-26	70.3	0.45	14.5	2.6	0.076	0.61	2.00	4.2	4.8	0.140
G-6	76.8	0.19	11.7	1.0	0.057	0.16	0.16	3.7	5.0	0.020
G-46	76.1	0.16	11.3	2.3	0.037	0.09	0.11	3.6	5.1	0.080
ARS	73.9	0.15	12.0	1.3	0.072	0.18	0.87	3.5	5.2	0.076
G-8	67.2	0.21	13.9	1.7	0.035	0.38	0.31	2.0	7.1	0.051
G-32	76.2	0.11	10.6	0.9	0.055	1.40	0.86	3.0	3.8	0.017
TTC	74.2	0.15	12.0	1.0	0.068	0.27	1.40	3.5	5.1	0.023
H9-77	71.2	0.30	14.5	2.0	0.062	0.50	1.40	4.2	4.9	0.120
G-11	82.0	0.07	9.8	0.4	0.024	0.07	0.06	0.5	6.0	0.013
TDW	70.1	0.11	11.9	0.9	0.053	0.68	1.70	0.6	5.7	0.016
G-1	69.4	0.16	12.7	1.2	0.039	0.68	1.70	2.3	3.8	0.024
G-81	66.8	0.68	15.5	3.5	0.072	0.63	1.60	4.2	4.8	0.190
G-47	66.5	0.80	16.2	5.1	0.081	1.70	4.00	3.7	2.9	0.190
G-43	64.0	0.53	15.9	4.0	0.068	0.82	3.10	3.7	3.5	0.140
G-55	62.8	0.19	14.7	1.5	0.046	3.30	4.00	0.4	1.8	0.072
G-84	62.5	0.52	15.4	2.4	0.089	0.38	1.10	4.8	5.2	0.073
G-31	71.5	0.36	13.3	2.4	0.063	0.50	1.20	2.9	5.7	0.082
A81-8	63.0	0.83	15.8	5.6	0.090	2.40	4.30	3.6	3.4	0.300
A81-12	48.5	1.70	16.4	11.8	0.170	6.10	8.50	3.2	0.8	0.290
A81-23	59.3	1.00	16.0	6.7	0.100	3.00	4.90	3.6	3.4	0.390
G-4	51.2	1.40	15.5	11.8	0.160	7.10	8.40	3.0	1.3	0.240
G-5	55.6	1.50	15.9	8.6	0.130	4.00	6.10	3.5	2.8	0.830
G-40	57.4	1.00	15.8	7.1	0.120	2.50	5.00	3.6	3.1	0.240

Sample identification:
G-7, G-23, G-24, G-48, G-51 & M-675 are Tbc;
G-15A, G-15B & G-26 are Tsp;
H9-77, TTC & G-32 are Tdc;
ARS, G-6 & G-46 are fbr;
G-8 is Cooney Tuff;
G-11 is the Sacaton quartz-latite squeeze-up;
G-1 & TDW are Fanney Rhyolite;
G-55 a white ash from Bull Basin;
G-31, G-43, G-47, G-81 & G-84 are miscellaneous felsic units;
A81-8, A81-12, A81-23, G-4, G-5 & G-40 are more mafic units.

Note: all iron is reported as Fe_2O_3

TABLE 2. Major element contents of rocks from the Mogollon-Datil volcanic field in weight percent.

Sample	Ba	Rb	Cu	Sol Zr	Sr	Zn	Cr	V	Ni	Ce	La
G-48	110	230	8	100	30	50	60	19	10	52	27
G-51	100	230	6	110	20	60	40	10	10	50	29
G-24	100	230	10	120	20	50	70	24	10	74	39
G-23	130	270	7	130	20	60	30	46	12	70	32
G-7	120	220	6	80	80	40	20	10	10	30	26
M-675	110	220	6	100	40	70	30	10	12	75	34
G-15B	650	180	10	110	150	30	20	27	13	74	50
G-15A	640	160	11	120	170	30	40	14	13	63	46
G-26	760	150	11	140	220	50	20	27	17	71	54
G-32	100	190	15	90	50	60	20	10	11	24	27
TTC	100	200	5	130	20	50	20	10	13	57	38
H9-77	700	180	10	120	170	60	30	26	17	93	55
G-6	100	280	4	170	20	50	20	10	10	270	31
G-46	100	220	13	270	20	70	60	10	16	150	73
ARS	100	240	12	120	30	30	50	10	10	58	42
G-8	450	300	10	100	90	50	20	170	9	78	39
G-11	100	400	6	100	30	20	120	10	10	20	20
TDW	100	220	8	90	90	20	20	10	13	52	4.1
G-1	180	230	10	150	370	40	20	17	10	52	40
G-81	1500	150	17	120	230	70	40	45	11	110	66
G-47	890	64	32	20	360	70	40	90	20	32	39
G-43	720	77	25	120	300	50	50	48	23	45	44
G-55	850	34	9	80	670	40	20	34	10	40	33
G-84	130	270	11	340	60	50	30	19	13	290	150
G-31	1200	180	14	130	190	40	70	34	15	80	51
A81-8	1100	100	40	400	410	80	170	94	50	100	70
A81-12	300	15	47	160	320	110	230	190	110	20	46
A81-23	910	89	34	400	450	90	120	110	50	92	68
G-4	210	13	100	140	260	120	210	180	150	20	42
G-5	1200	63	41	400	600	110	120	150	67	100	74
G-40	790	100	35	260	400	80	70	180	39	53	48

Examination of the chemical variances against silica shows that Al_2O_3 is high and has a slight negative slope for silica contents below 65% and a more pronounced negative slope for higher silica rocks. Fe, Mg, Ti, Mn and Ca oxides have a negative slope for the mafic rocks, and relatively flat and scattered plots above 65% silica. Trace elements Zr, Zn, Cr, Cu, V and Ni, have negative slopes in the sub-65% silica range, but scatter in a fairly flat-lying pattern above that. Ba, Ce and La have scatter plots with no obvious trend, with the rare earth elements plotting roughly horizontally, and Ba showing much higher scatter in the mid-range in silica. For the purpose of PER denominators, the comparatively horizontal trend of trace-element plots in the plus-65% silica range were considered adequate. Much of this scatter is experimental error in the determination of small absolute contents of the trace elements.

Using the Cox et al. (1979) alkali-silica, or the LeBas et al. (1986) total alkali-silica classifications, the Davis Canyon, Shelley Peak and Bloodgood Canyon tuffs are all rhyolites, and plot in the sub-alkaline field of Irvine and Barager (1971). Ratté et al. (1984) used the De la Roche et al. (1980) volcanic classification to place the Davis Canyon and Bloodgood Canyon tuffs in the alkali rhyolite category, and the Shelley Peak Tuff in the rhyolite class. As there is not a large difference in the chemistry between the three ash flows, changes in their parent magma would be expected to be relatively small. Such small changes should nevertheless show up as linear trends in the PER diagrams if they reflect removal of one or more minerals from the melt.

PEARCE ELEMENT RATIOS

Russell and Nicholls (1988) summarized the Pearce element ratios most suitable to various petrologic arguments. The placement of the required fraction can be done on either the ordinate or abscissa. For one or two phase segregation, one axis (usually the Y axis) used is Si/n, where n is the conserved element (Zr, Cu, Ti, La or Ce in this study) used as the denominator for the abscissa and ordinate. The other axis (usually the X axis) has the following factors, divided by n: for olivine (OL), 0.5(Mg+Fe); for plagioclase (PL), 2Na+Al; and for clinopyroxene (CPX), 2Ca+Na-Al. For two minerals concurrently involved in fractionating, the following, divided by n are used as the Y axis: OL+PL 0.5(Mg+Fe)+2Ca+3Na; PL+CPX 2Ca+3Na; and OL+CPX 0.5(Fe+Mg)+1.5Ca.

For three minerals (Russell et al., 1990) Y is (OL+CPX+PL)/n or [1.5Ca+0.25Al+0.5FM+2.75Na]/n. In all of these plots, fractionation of the indicated species will produce a line with a slope of 1.0. Another way of testing for these minerals is to use the axes Al/n and {2Ca+Na}/n (Russell and Nicholls, 1988). Here a slope of 1.0 reflects plagioclase involvement; if Al/n is the abscissa a vertical line indicates CPX, the actual slope is equal to the {CPX+PL}/PL ratio, and OL has no effect on the slope. If Al/n is the ordinate, then CPX fractionation alone will be horizontal, or a slope of ∞.

Plots and regression calculations were made using Ti and the trace elements Cu, soluble Zr, Ce and La for all the analyzed samples of Bikerman et al. (1992) and for various subsets such as the three major ash flows, or of all the high silica rocks using mainly the program Igpet 3.2 (Carr, 1992). The parameter of {4(Ca+Na)+0.5(Fe+Mg)}/n as the Y axis, selected by Bradshaw (1992) as being especially suited for silica-rich rocks, was made by summing two available Igpet 3.2 PER parameters (2Ca+3Na) and (2Ca+Na) with the also available 0.5(Mg+Fe).

Slight variations in the PER plots and their regressions occur as the element of the denominator is changed. Intercepts of the regression lines reflect the absolute abundances of the trace elements and so are not considered here. Intercepts of zero violate one of the criteria for PERs, in which case the plot is not used. Table 3 shows a series of sample calculations for the various denominator elements. There are slight differences in the slopes, but the petrologic interpretations are not significantly affected by changing the element used. As the Mogollon-Datil region is peripheral to copper mining districts, Cu was chosen as the element most commonly used in PER denominators in this study. The region's copper deposits are Laramide or older, and hence they, or their progenitors, are likely to be represented in the crust involved in the generation of the magma parent to the ash flows.

Examined first is the idea that a single phase fractionated from the parent magma. Using the axes for olivine (Fig. 3) and for clinopyroxene (Fig. 4) as listed above, plots of 15 points (6 for Bloodgood Canyon Tuff, and 3 each for Shelley Peak, Davis Canyon and flow-banded rhyolite

TABLE 3. Comparison of different elements as PER denominators. All were used in the PER test of (2Ca+Na)/n vs. Al/n.

n=	slope	R=	R^2=	t=
sol Zr	1.23	0.779	0.61	3.73
Cu	1.44	0.932	0.87	7.73
Ce	1.60	0.977	0.95	13.65
La	1.66	0.841	0.71	4.67
Ti	1.43	0.931	0.87	8.06

Note: R, R^2 and t are statistical functions for goodness of fit, square of the goodness of fit, and t- test, respectively.

analyses) yield calculated slopes of 44.8 and 11.1 respectively. These values are far from the postulated value of 1.0, indicating that neither of these minerals fractionating by itself could produce the observed trends. For plagioclase (Fig. 5) the plot of Si/Cu vs (2Na+Al)/Cu gives a calculated slope of 2.67±0.34 for 15 points, and similar values for subsets for each of the ash flows. Plagioclase fractionation is within reason.

Next, examining the pairs of minerals using the appropriate axes of Russell and Nicholls (1988) shows that either olivine + plagioclase (Fig. 6) or clinopyroxene + plagioclase (Fig. 7) give slopes of about 3.1±0.33, or roughly the same as for plagioclase alone. As olivine is unlikely to be an important factor in rhyolite magmatism, ferro-magnesian partition modeling using clinopyroxene is preferable. To determine the molar proportion of plagioclase to pyroxene the three-phase plot of Russell and Nicholls (1988) is used, where the slope of the regression line gives the PL/(PL+CPX) ratio. A slope = 1 is simple plagioclase removal, and with the axes used, a zero slope is pure CPX removal. In the 15-point set (Fig. 8) this value is 0.67, or 67% plagioclase removal to 33% clinopyroxene. The same calculation for each caldera gives 80% PL out for the Gila Cliff Dwellings Caldera tuffs and 55% PL out for the Bursum Caldera. The presence of green clinopyroxene in the younger Shelley Peak tuff is consistent with removal of plagioclase from its parent magma.

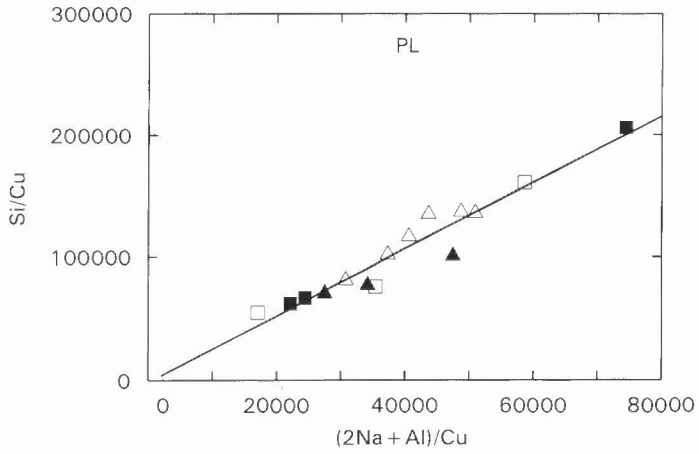

FIGURE 5. Plagioclase fractionation; symbols and line as in Fig. 4.

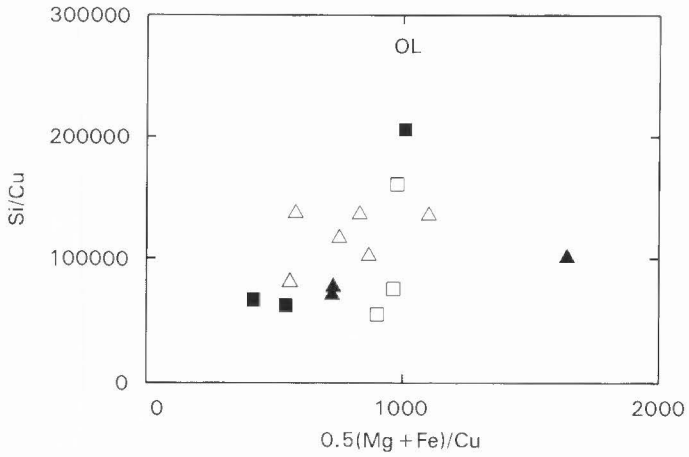

FIGURE 3. Olivine fractionation using the axes suggested by Russell and Nicholls (1988). Symbols are Tbc - open triangles; Tsp - filled triangles; Tdc - open squares; fbr - filled squares

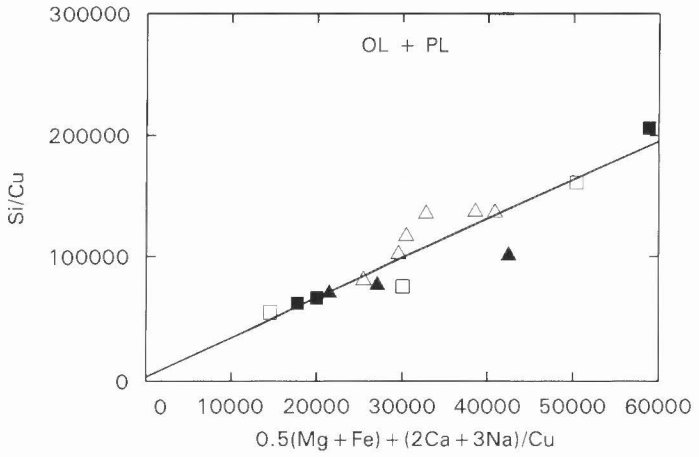

FIGURE 6. Olivine + plagioclase fractionation; symbols and line as in Fig. 4.

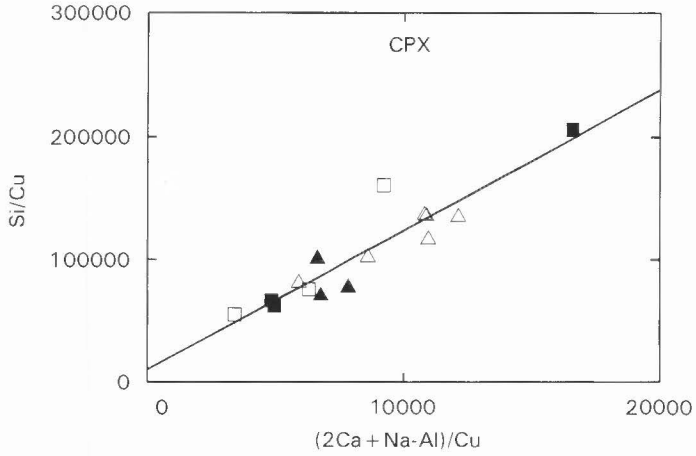

FIGURE 4. Clinopyroxene fractionation, symbols as in Fig. 3. Line is regression line calculated by Igpet 3.2 (Carr, 1992)

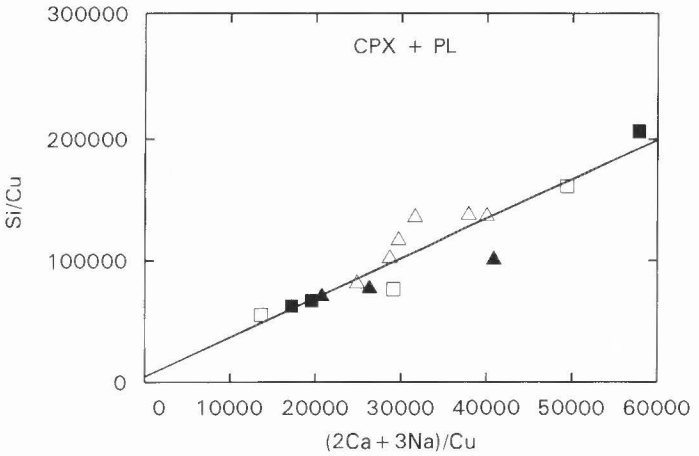

FIGURE 7. Clinopyroxene + plagioclase; symbols and line as in Fig. 4.

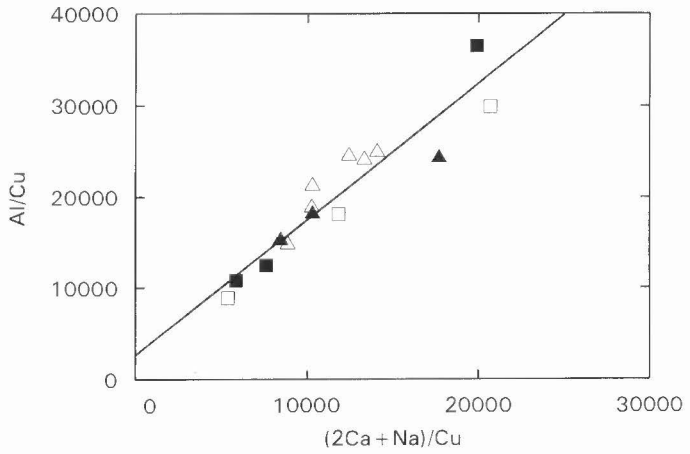

FIGURE 8. Three phase diagram with plagioclase (slope of 1) and clinopyroxene (slope ∞, horizontal); symbols and line as in Fig. 4.

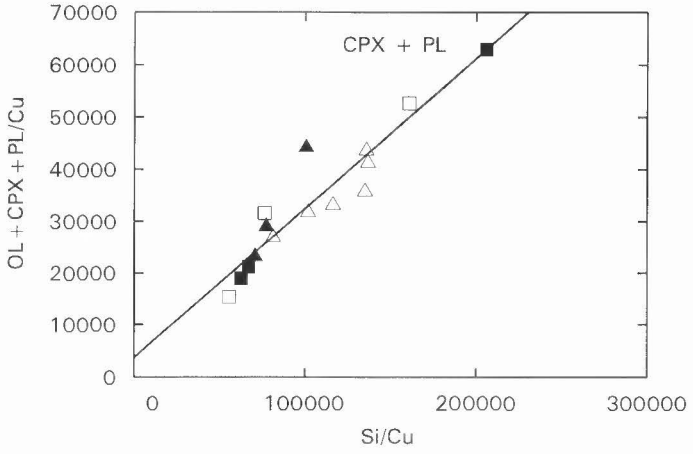

FIGURE 9. OL + CPX + PL diagram; symbols and line as in Fig. 4.

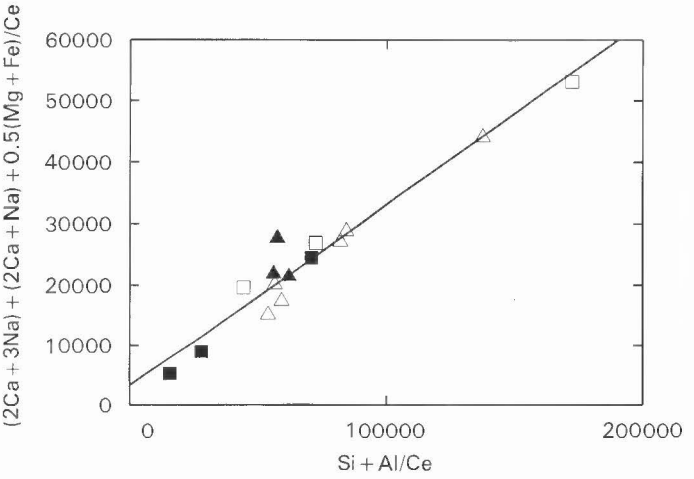

FIGURE 10. PER diagram after Bradshaw (1992); symbols and line as in Fig. 4. Ce is used rather than Cu because the regression value for Ce is 0.964 compared to 0.855 for Cu.

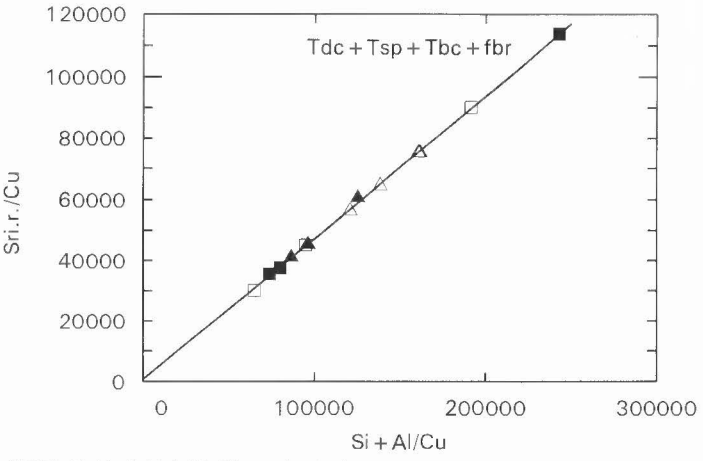

FIGURE 11. Initial $^{87}Sr/^{86}Sr$ ratio [Sr i.r.] treated as a PER factor and plotted against [Si+Al]/n. Symbols and line as in Fig. 4.

For the [OL+CPX+PL]/n diagram (Fig. 9) the slopes are less than 1.0, indicating that other phases were also involved. As sanidine is a common mineral in these ash flows, adding K-spar to the mix of minerals was attempted. In the plot suggested by Bradshaw (1992) (Fig. 10) fractionation of K-spar appears as a horizontal displacement because only Al and Si change, and enstatite has a slope of 0.5, plagioclase a slope of 1, and clinopyroxene a slope of 2.25. The 15 point regression line has a slope of 0.31 using Cu or 0.30 using Ce as the denominator. Ce was selected for use because of a better statistical fit of the points to the regression line. The slopes for the Gila Cliff Dwellings ash flows are 0.26, whereas the Bursum caldera ash flow has a slope of 0.33. These figures hint that the Bursum caldera chamber had a slightly greater pyroxene and plagioclase extraction.

The PER Assemblage Test Diagram program (Stanley and Russell, 1989) suggests using Si/n as the X axis, and [0.5Al+Fe+Mg+Ca+2.5Na+2.5K]/n as the Y axis, for a line that gives a slope of 1 for fractionation of any of the following: K- spar, AN, AB DP, HD or EN. Such plots were made, and lines with a slope of 0.24 for n=Cu, and of 0.26 for n=Ce resulted. Errors on each of the slopes are about 5%, and the R squared values are 0.909 and 0.969, respectively. Again the model was not definitive for these minerals, implying that some other phase(s) were involved.

An interesting correlation was found between the initial $^{87}Sr/^{86}Sr$ ratio and either Si or Al or both. Plots of initial $^{87}Sr/^{86}Sr$ against either SiO2 or Al2O3 produced essentially horizontal linear scatter plots, which resemble the plots of the Sr ratio against Si/Cu, Al/Cu and [Si + Al]/Cu. However, if the initial Sr ratio is treated as a PER parameter, using the initial $^{87}Sr/^{86}Sr$/Cu ratio produced tight sloping lines, especially against [Si+Al]/Cu (Fig. 11), an observation which holds for other conserved element denominators as well. The Sr ratios did not work as PER denominators themselves, emphasizing their non- conservation in the melt. The only caveat to any petrologic interpretation is that the intercepts are near zero, hence possibly spurious. If the lines have meaning, it may be that the isotopic ratios in the magma chamber parallel the mineral fractionation, possibly indicating a Rb-zoned magma chamber. The AFC-derived model for the origin of the ash flows based on the $^{87}Sr/^{86}Sr$ and $^{143}Nd/^{144}Nd$ data (Bikerman et al., 1992), could well produce a stratified magma chamber.

CONCLUSIONS

The chemical and $^{87}Sr/^{86}Sr$ data used in the PER models are consistent with a reasonably well mixed rhyolite magma fractionating pyroxene and plagioclase feldspar. Fractionation of 80:20 PL:CPX is found for the Gila Cliff Dwellings rhyolites, supported by the petrographic evidence of clinopyroxenes in the Shelley Peak Tuff, and of 55:45 in the Bloodgood Canyon Tuff from the Bursum caldera. Orthopyroxene fractionation could have been a major factor in the Bursum caldera also. The deviations from the simple fractionation used could be caused by biotite removal, which was not indicated by the PER models used.

The PER and isotopic data for the Davis Canyon, Shelley Peak and Bloodgood Canyon tuffs, together with the associated flow-banded rhyolites, can be explained by an evolving magma chamber derived

from a mix of primary mantle-derived magma and some crustal contaminant, such as the AFC model which best fit the $^{143}Nd/^{144}Nd$ and $^{87}Sr/^{86}Sr$ determinations (Bikerman et al., 1992).

$^{87}Sr/^{86}Sr$ initial/n in the rocks plots linearly against [Al+Si]/n. If the near-zero intercept is significant, the line can be construed as a genetic relationship, rather than a stoichiometric one between the numerator parameters. The geological import of this is that more alkali-feldspar-rich rocks would have higher Al+Si, and more Rb in their source. A clearer understanding of the processes and sources leading to the rhyolites could be gained if better data on the pre-existing crust were available. Searching for crustal and mantle xenoliths has not been successful so far, but more field and laboratory time is needed.

ACKNOWLEDGMENTS

Thoughtful and helpful reviews by E. G. Lidiak and C.H. Shultz, and field support from the New Mexico Bureau of Mines and Mineral Resources, are gratefully acknowledged.

REFERENCES

Bikerman, M., 1989, Rb, Sr, Rb-Sr, and isotopic Sr values for volcanic rocks from the southwestern Mogollon-Datil volcanic field, New Mexico: New Mexico Geology, v. 11, p. 76-83.

Bikerman, M., Bell, K. and Card, J.W., 1992, Strontium and neodymium isotopic study of the western Mogollon-Datil volcanic region, New Mexico, USA: Contributions to Mineralogy and Petrology, v. 109, p. 459-470.

Bornhorst, T.J., 1980, Major- and trace-element geochemistry and mineralogy of Eocene to Quaternary volcanic rocks of the Mogollon-Datil volcanic field, southwestern New Mexico [PhD dissertation]: Albuquerque, University of New Mexico, 500 p.

Bornhorst, T.J., 1985, Abundance and variability of selected lithophile elements in high-K rhyolitic rocks, Mogollon-Datil volcanic field, southwestern New Mexico: *in* Taylor, R.P. and Strong, D.F., eds, Granite-related mineral deposits: Canadian Institute of Mining Conference, Halifax, p. 25-31.

Bradshaw, T.K., 1992, The adaptation of Pearce element ratio diagrams to complex high silica systems: Contributions to Mineralogy and Petrology, v. 109, p. 450-458.

Carr, M.J., 1992, Igpet 3.2. Terra Softa Inc., Somerset NJ, 46 p.

Cox, K.G., Bell, J.D. and Pankhurst, R.J., 1979, The Interpretation of Igneous Rocks: Allen and Unwin, London, 450 p.

De la Roche, H., Leterrier, J., Grandclaude, P. and Marchal, M., 1980, A classification of volcanic and plutonic rocks using R1R2- diagram and major element analyses - its relationship with current nomenclature: Chemical Geology, v. 29, p. 183-210.

DePaolo, D.J., 1981, Trace element and isotopic effects of combined wall rock assimilation and fractional crystallization: Earth and Planetary Science Letters, v. 53, p. 189-202.

Elston, W.E., 1984, Mid-Tertiary ash-flow cauldrons, southwestern New Mexico: Journal of Geophysical Research, v. 89, p. 8733-8750.

Elston, W.E. and Northrop, S.A., eds, 1976, Cenozoic volcanism in southwestern New Mexico: New Mexico Geological Society, Special Publication 5, 151 p.

Irvine, T.N. and Barager, W.R.A., 1971, A guide to the chemical classification of the common volcanic rocks. Canadian Journal of Earth Sciences, v. 8, p. 523-548.

LeBas, M.J., LeMaitre, R.W., Streckeisen, A. and Zanettin, B., 1986, A chemical classification of volcanic rocks based on the total alkali silica diagram: Journal of Petrology, v. 27, p. 745- 750.

Marvin, R. F., Naeser, C. W., Bikerman, M., Mehnert, H. H. and Ratté, J.C., 1987, Isotopic ages of post-Paleocene igneous rocks within and bordering the Clifton 1°X2° quadrangle, Arizona-New Mexico: New Mexico Bureau of Mines and Mineral Resources, Bulletin 118, 63 p.

McIntosh, W.C., Kedzie, L.L. and Sutter, J.F., 1991, Paleomagnetism and $^{40}Ar/^{39}Ar$ ages of ignimbrites, Mogollon-Datil volcanic field, southwestern New Mexico, New Mexico Bureau of Mines and Mineral Resources, Bulletin 135, 79 p.

McIntosh, W.C., Chapin. C.E., Ratté, J.C. and Sutter, J.F., 1992, Time-stratigraphic framework for the Eocene-Oligocene Mogollon-Datil volcanic field, southwest New Mexico: Geological Society of America Bulletin, v. 104, p. 851-871.

Nicholls, J., 1988, The statistics of Pearce element ratios and the Chayes closure problem. Contributions to Mineralogy and Petrology, v. 99, p. 11-24.

Pearce, T.H., 1968, A contribution to the theory of variation diagrams: Contributions to Mineralogy and Petrology, v. 19, p. 142-157.

Pearce, T. H., 1987, The identification and assessment of spurious trends in Pearce-type variation diagrams: a discussion of some statistical arguments: Contributions to Mineralogy and Petrology, v. 97, p. 529-534.

Ratté, J.C. and Grotbo, T., 1979, Chemical analyses and norms of 81 volcanic rocks from part of the Mogollon-Datil volcanic field, southwestern new Mexico: U.S. Geological Survey, Open-file Report 79-1435, 33 p.

Ratté, J.C., Marvin, R.F., Naeser, C.W. and Bikerman, M., 1984, Calderas and ash flow tuffs of the Mogollon Mountains, southwestern New Mexico: Journal of Geophysical Research, v. 89, p.8713-8732.

Russell, J.K. and Nicholls, J., 1988, Analysis of petrologic hypotheses with Pearce element ratios: Contributions to Mineralogy and Petrology, v. 99, p. 25-35.

Russell, J.K., Nicholls, J., Stanley, C.R. and Pearce, T.H., 1990, Pearce element ratios – a paradigm for testing hypotheses: EOS, v. 71, p. 234-6, 246-7.

Stanley, C.R. and Russell, J.K., 1989, Petrological hypothesis testing with Pearce element ratio diagrams: derivation of diagram axes: Contributions to Mineralogy and Petrology, v. 103, p. 78-89.